Autonomous Mobile Robot Control Using Kinematics and Dynamics Based Approaches - An Experimental Analysis

D.S. Necsulescu, V. Lonmo, B. Kim, E, Droguet
Department of Mechanical Engineering
University of Ottawa
Ottawa, Ont., K1C 5R5, Canada

Abstract - Motion control of wheeled mobile robots is based on kinematic or dynamic models and has to take into account nonholonomic constraints resulting from ideal rolling requirement. In order to achieve autonomy in motion, the trajectory has to be generated in real time and has to be corrected in case of reaching a constraint limit, as for example servomotor torque saturation limit. In this paper, results of experimental verification of kinematics and dynamics based control strategies are reported and analysed from the point of view of computational complexity versus performance limitations.

I. INTRODUCTION

Wheeled mobile robots under ideal requirements are known to be difficult to control for centre of mass position and body orientation given that the nonholonomic constraints reduce the number of degrees of freedom. For example, a wheeled mobile robot moving on a flat surface has only two degrees of freedom and cannot be stabilized by a smooth state feedback [1]. Given the stabilization problem, discontinuous and time varying control laws have been proposed [1,2]. Also, for a tricycle with front wheel steering and driving, an artificial holonomic constraint approach was proposed such that smooth state feedback is used for front wheel angular speed and steering angle and an open loop control for body orientation [3]. The state feedback loop enclosed also an input-output linearization of the mobile robot dynamics [4].

The smoothness condition for input-output linearization requires verification of bounded variables and in particular of the servomotor torques versus their saturation limits [3,4]. Predictive control has been used for a holonomic system subject to feedback linearization with bounded inputs [5].

In this paper, these new results in dynamic-based control are verified experimentally and compared to the computationally less intensive approach based on kinematic model only. A short presentation of the experimental mobile robot is followed by the description of the control strategies and by the analysis of the experimental results.

II. EXPERIMENTAL MOBILE ROBOT

The mobile robot shown in fig. 1 has 0.51 x 0.51 x 0.53m and weights 24.5 Kg. It has a tricycle configuration with front wheel driving and steering. The DC servomotors have 75.1:1 planetary gears and have a torque output of maximum 10 Nm.

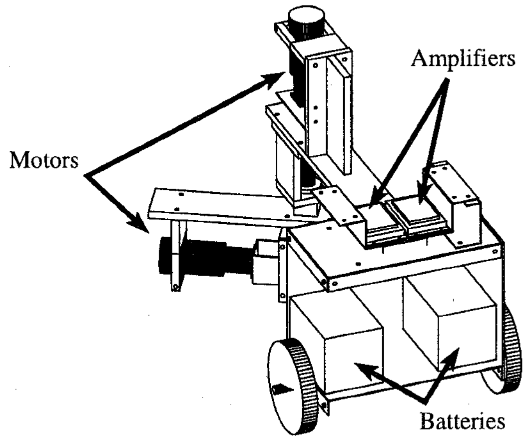

Fig.1 Major Components of the mobile robot

Power for the motors is supplied by two 12 V, 10 Ah batteries connected in series. The dSPACE controller (fig. 2) is DSP based(TMS 320C30) and contains D/A and incremental encoder boards [6]. Each optical encoder has 1000 steps per revolution at motor shaft resulting in 75100 steps per revolution for output shaft. The identification of dry friction torques gave approximately 1.1 Nm.

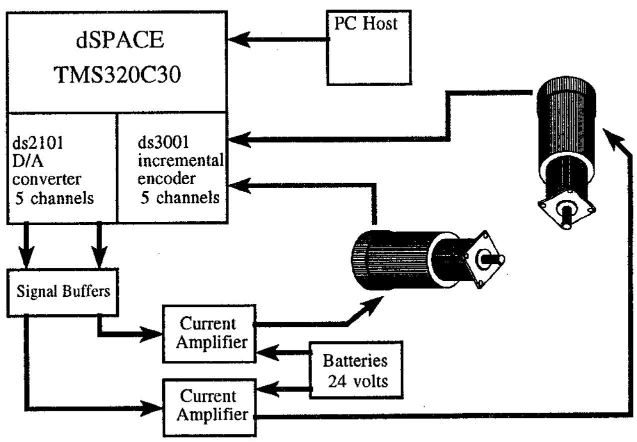

Fig.2 Electrical Components

III. DYNAMIC MODEL OF THE MOBILE ROBOT

The reference frames for the mobile robot are shown in fig.3 where δ,θ are the steering angle and the absolute orientation angle, respectively.

The dynamic model is given by,[3,4]

$$\begin{bmatrix}\dot{\omega}_\delta\\ \dot{\omega}_1\end{bmatrix}=\begin{bmatrix}f(\omega_1,\omega_\delta,\delta,\theta)\\ F(\omega_1,\omega_\delta,\delta,\theta)\end{bmatrix}+Ad\begin{bmatrix}\tau_d\\ \tau_s\end{bmatrix} \tag{1}$$

where, τ_d, τ_s are the driving and steering torques, respectively, and $\dot{\omega}_1$, $\dot{\omega}_\delta$ are the driving and steering angular accelerations, respectively (i.e. $\dot{\omega}_\delta=\ddot{\delta}$),

$$f(\omega_1,\omega_\delta,\delta,\theta)=\frac{r_1}{bD}\omega_1\omega_\delta[r_l^2\{\frac{l}{2b}Q_1(\sin^2(\delta)-\cos^2(\delta))+(Q_3-Q_4)\sin(\delta)\cos(\delta)\}\sin(\delta)-D\cos(\delta)] \tag{2}$$

$$F(\omega_1,\omega_\delta,\delta,\theta)=-\frac{r_1^2}{D}\omega_1\omega_\delta[\frac{l}{2b}Q_1(\sin^2(\delta)-\cos^2(\delta))+(Q_3-Q_4)\sin(\delta)\cos(\delta)] \tag{3}$$

$$Ad=\begin{bmatrix}-\frac{r_1}{bD}\sin(\delta) & \frac{1}{J_1}+\frac{r_1^2}{b^2D}\sin^2(\delta)\\ \frac{1}{D} & -\frac{r_1}{bD}\sin(\delta)\end{bmatrix} \tag{4}$$

$$D=I_1+r_1^2[Q_4\cos^2(\delta)+Q_3\sin^2(\delta)-\frac{1}{b}Q_1\cos(\delta)\sin(\delta)]$$

Complete equations used for deriving Q_1, Q_2, Q_3, Q_4 and definitions of r_1, b, c, J_1,are given in [7].

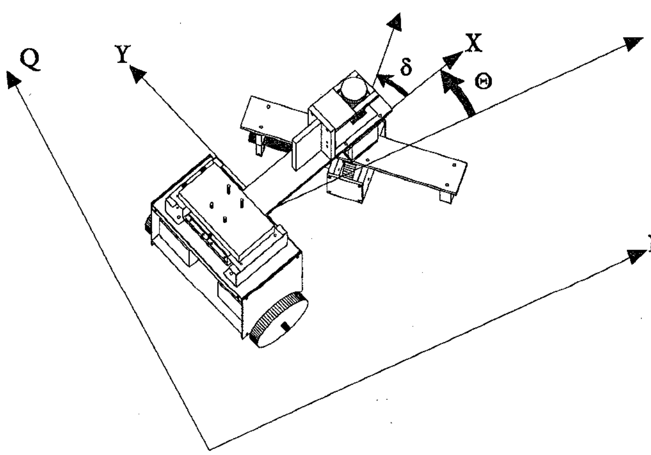

Fig. 3 Reference frames for the mobile robot

IV. TORQUE SATURATION AVOIDANCE FOR A MOBILE ROBOT MOVING ON A HORIZONTAL PLANE

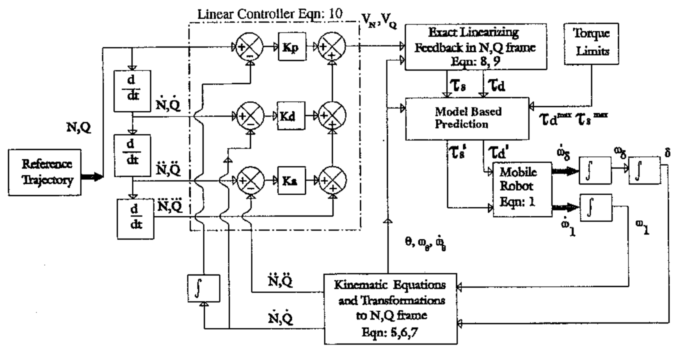

Fig. 4 Block diagram of the dynamics based controller for the horizontal plane motion of a mobile robot with torque saturation avoidance

The mobile robot represented in fig. 1 is analysed for the case of horizontal planar motion with actuator torque saturation avoidance. The block diagram of the dynamics based control system is shown in fig. 4 and contains an exact linearizing feedback controller, whose smoothness condition is achieved by a model based prediction.

The equations corresponding to the blocks of fig. 4 are the following:

Kinematic equations are:

$$\dot{N}=r_1\omega_1(\cos\delta\cos\theta-\frac{c}{b}\sin\delta\sin\theta) \tag{5}$$

$$\dot{Q}=r_1\omega_1(\cos\delta\sin\theta+\frac{c}{b}\sin\delta\cos\theta) \tag{6}$$

$$\omega_\theta=\dot{\theta}=\frac{1}{b}r_1\omega_1\sin\delta \tag{7}$$

Linearizing Feedback Controller is given by,

$$\tau=M^{-1}U \tag{8}$$

$$W=\Delta^{-1}(V-\Delta_0) \tag{9}$$

where:

$$\tau=\begin{bmatrix}\tau_d\\ \tau_s\end{bmatrix}$$

$$M=\begin{bmatrix}1 & -\frac{r_1}{b}\sin(\delta)\\ 0 & 1\end{bmatrix}$$

$$U=\begin{bmatrix}u_1\\ w_2\end{bmatrix}\quad W=\begin{bmatrix}\dot{u}_1\\ \tau_s\end{bmatrix}\cdot\quad V=\begin{bmatrix}V_N\\ V_Q\end{bmatrix}$$

$$\Delta(\delta,\theta,\omega_1) = \begin{bmatrix} r1\dfrac{A1}{Den(\delta)} & -\left(A_3 + A_1\dfrac{Num(\delta)}{Den(\delta)}\right)\dfrac{r_1\omega_1}{J_1} \\ r1\dfrac{A_2}{Den(\delta)} & -\left(A_4 + A_2\dfrac{Num(\delta)}{Den(\delta)}\right)\dfrac{r_1\ \omega_1}{J_1} \end{bmatrix}$$

$$\Delta_O(\delta,\ \theta,\ \omega_1,\ \omega_\delta,\ \omega_\theta,\ \dot{\omega}_1) = \begin{bmatrix} \Delta_{ON}(\delta,\ \theta,\ \omega_1,\ \omega_\delta,\ \omega_\theta,\ \dot{\omega}_1) \\ \Delta_{OQ}(\delta,\ \theta,\ \omega_1,\ \omega_\delta,\ \omega_\theta,\ \dot{\omega}_1) \end{bmatrix}$$

$$\begin{aligned} \Delta_{ON} = {} & r_1 A1C2 - r_1\omega_1 A3C1 + 2r_1\dot{\omega}_1(-A2\omega_\theta - A3\omega_\delta) \\ & - r_1\omega_1\omega_\theta(A1\omega_\theta - A4\omega_\delta) - r_1\omega_1\omega_\delta(-A4\omega_\theta + A1\omega_\delta) \\ & - r_1\omega_1 A3\dot{\omega}_\theta \end{aligned}$$

$$\begin{aligned} \Delta_{OQ} = {} & r1A2C2 - r_1\omega_1 A4C1 + 2r_1\dot{\omega}_1(A1\omega_\theta - A4\omega_\delta) \\ & + r_1\omega_1\omega_\theta(-A2\omega_\theta - A3\omega_\delta) - r_1\omega_1\omega_\delta(A3\omega_\theta + A2\omega_\delta) \end{aligned}$$

$$C1 = \frac{r_1}{b_1}\sin(\delta)\dot{\omega}_1 - \frac{r_1}{b_1}\omega_1\omega_\delta\cos(\delta)$$

$$\begin{aligned} C2 = {} & \frac{Num(\delta)}{Den(\delta)}\omega_1 C1 - \frac{Num'(\delta)\ \omega_1 + Num(\delta)\dot{\omega}_1}{Den(\delta)}\omega_\delta \\ & - \frac{Den'(\delta)}{Den(\delta)}\omega_1 - \omega_1(\omega_\theta + \omega_\delta)^2 \end{aligned}$$

$$A1 = \cos(\delta)\cos(\theta) - \frac{c}{b}\sin(\delta)\sin(\theta)$$

$$A2 = \cos(\delta)\sin(\theta) + \frac{c}{b}\sin(\delta)\cos(\theta)$$

$$A3 = \sin(\delta)\cos(\theta) + \frac{c}{b}\cos(\delta)\sin(\theta)$$

$$A4 = \sin(\delta)\sin(\theta) - \frac{c}{b}\cos(\delta)\cos(\theta)$$

and C1, C2, Num(δ), Den(δ), Num'(δ), Den'(δ) are derived in [3,4].

Linear Controller is given by,

$$V = K_p(P_d - P) + K_d(P_d^{(1)} - P^{(1)}) + K_a(P_d^{(2)} - P^{(2)}) + P_d^{(3)} \quad (10)$$

where,

$$V = [\ V_N \quad V_Q]^T \qquad P = [\ N \quad Q\ ]^T$$

V_N, V_Q are the resolved jerks.

The one-step (Δt) model based prediction ,shown in fig. 5, compares the input torque commands τ_d and τ_s with saturation torque limits and reduces any torque greater than the saturation limit by its saturation limit resulting in a new torque command vector τ_{safe}. For this τ_{safe} , the new (8),(9) written as,

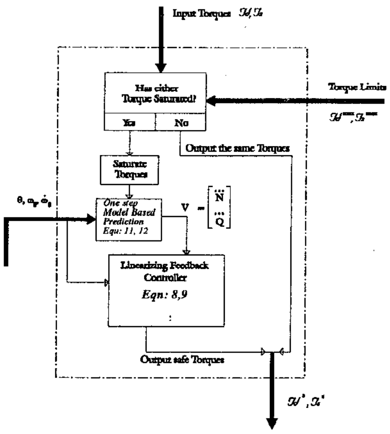

Fig. 5 Block diagram of the model based prediction and recalculation of the feasible torques for avoiding torque saturation

$$U = M\ \tau_{safe} \quad (11)$$

$$V_{new} = \Delta W + \Delta_0 \quad (12)$$

where M, Δ, Δ_0 were assumed equal to their values for previous resolved jerks given by the linear controller (10) (fig. 4). If M, Δ, Δ_0 vary significantly with the change from the old to the new V, i.e.,functions of V, an iterative approach can be used to obtain the set of commands V and τ consistent with the path and within torque saturation limits. The new jerk commands vector V_{new} is used as input to the linearizing feedback controller for recalculating M, Δ, Δ_0, W and τ using (8),(9) (fig.5). If the resulting torque commands are within saturation limits, they are used as τ_d^s, τ_s^s inputs to the mobile robot servomotors (fig. 4). If not, the iterations using the model based prediction of fig. 5 are continued. In simulations this approach converged fast. In experiments it is preferable to use very short steps Δt such that M, Δ, Δ_0 vary insignificantly with the changes in V. In this case the model based prediction is reduced to an algebraic dependence between τ and V in (10) and (11) and can be solved in one iteration. The block diagram for the model based prediction is given in fig. 5, shown for one iteration in order to keep the block diagram simple.

V. KINEMATICS AND DYNAMICS BASED CONTROLLER

Kinematics based controller is shown in fig. 6. Front wheel angular speed ω_1 and steering angle δ are controlled by a proportional and, respectively, proportional derivative control laws in order to follow the reference trajectory given in operational space N-Q. The position and orientation of the mobile robot are obtained by odometry using front wheel angular speed and steering angle measurements. Servomotor torques τ_d and $_s\tau$ are limited by software to conventional saturation torques chosen lower than actual saturation torques.

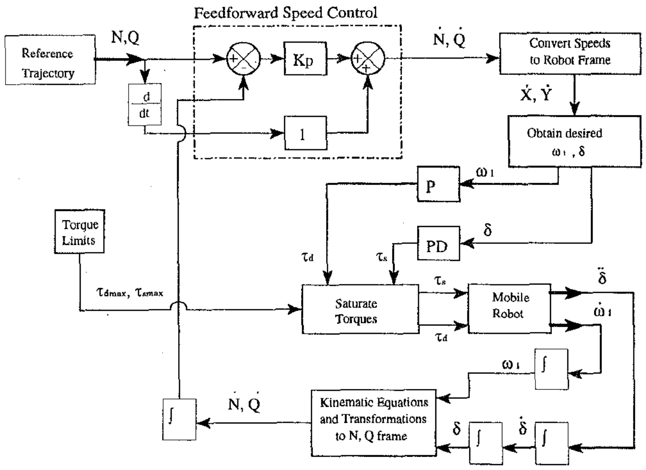

Fig. 6 Block diagram of the system using the Kinematic based controller

Dynamics based controller is based on the block diagram shown in fig. 4 and uses the dynamic model of this mobile robot given by (1).

Exact linearizing feedback and model based prediction are used to transform jerk commands V_N, V_Q into torque commands to the servomotors which avoid to reach saturation limits (fig. 5) [3,4]. Again, odometry is used to obtain operation space position, speed, $\dot{N}$, $\dot{Q}$, and $\ddot{N}$, $\ddot{Q}$ based on front wheel angular speed ω_1 and steering angle δ measurements. A linear controller PDD given by (10) generates the resolved jerks V_N and V_Q given the reference trajectory.

VI. EXPERIMENTAL RESULTS

The kinematics and dynamics based control schemes were verified for a discontinuous(step) path and a sinusoidal path. Both control schemes tracked the sinusoidal path in a similar fashion. The kinematics based controller had to have the gains retuned for each important change of the path while the dynamics based controller which performed well for all paths using the same gains.

Fig. 7 and 8 shows the results for the discontinuous (step) reference path (dotted lines in fig. 7a and 8a). The kinematics based controller was unable to track the path (plain line in fig 7a), reached a $2\pi/3$ steering angle and stopped (fig. 7a). Fig. 7c shows high oscillations of the steering torque for the case of actual saturation torque limits (dotted line) while for the lower saturated torque limits of 4 Nm (obtained by settings in control software), the controller operates most of the time at torque limit (plain line in fig. 7b and c) of approximately 10 Nm. The dynamics based controller tracked the reference path (fig. 8a), keeping both driving and steering torques within a limited range, lower than saturation limits, in both cases, for actual saturation limits of approximately 10Nm (dotted lines in fig. 8b and c) and lower saturation limits of 4 Nm, set by control software (plain lines in fig. 8b and c).

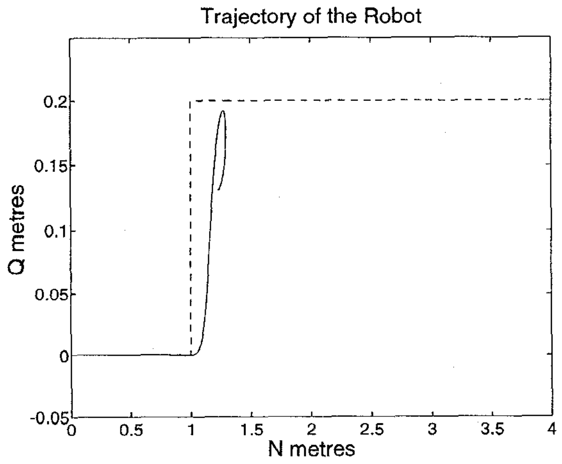

(a)

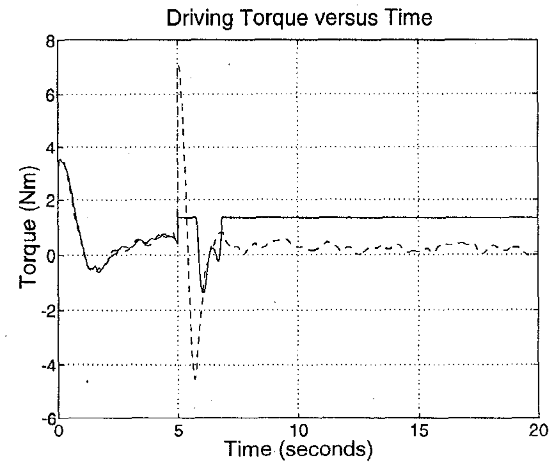

(b)

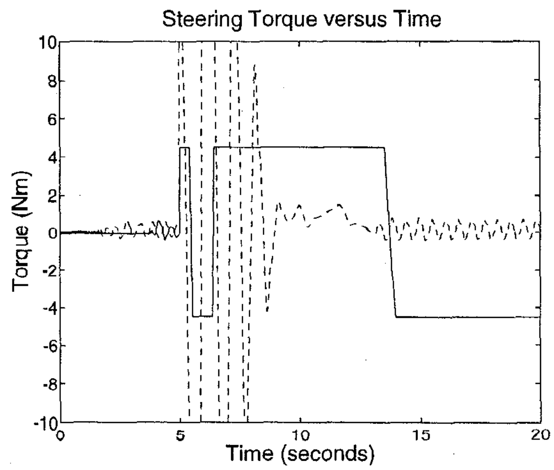

(c)

Fig. 7 Experimental Results using a Kinematics based controller
a) Trajectory with torque saturation
b) Driving Torque versus time
c) Steering Torque versus time

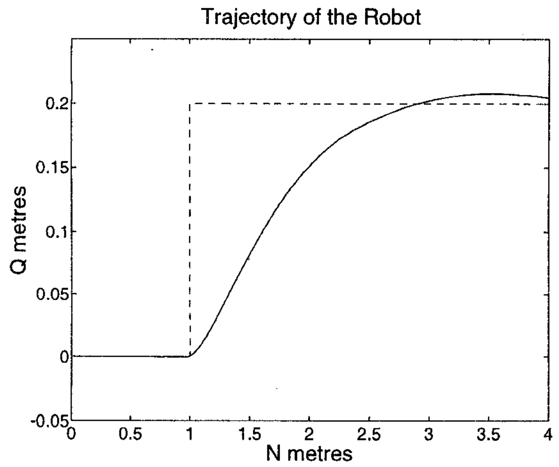

(a)

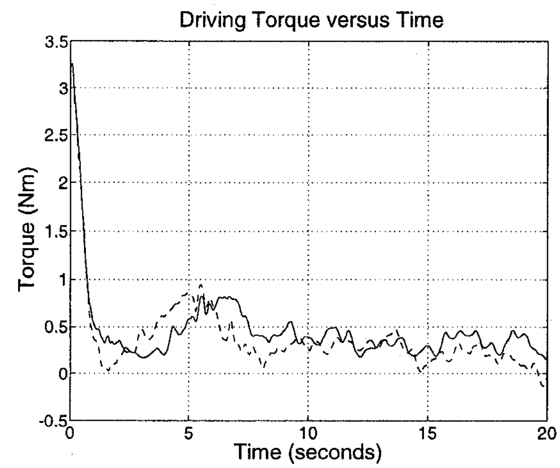

(b)

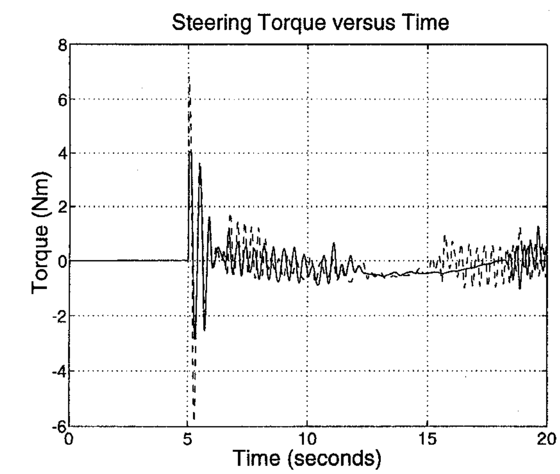

(c)

Fig. 8 Experimental Results using a Dynamics based controller
a) Trajectory with torque saturation
b) Driving Torque versus time
c) Steering Torque versus time

VII. CONCLUSIONS

The experimental results confirm that, while more intensive computationally, dynamics based controller is more suitable in achieving autonomous motion for mobile robots given that the controller gains do not have to be retuned for various reference paths and that servomotor torque saturation limits are not reached as a result of the model based prediction used in conjunction with the linearizing feedback controller.

REFERENCES

[1] C. Samson, "Velocity and Torque Feedback Control of a Nonholonomic Cart", in *Advanced Robot Control*, C. Canudas de Wit(Ed), Springer Verlag, 1991, pp.125-151

[2] C. Canudas de Wit, O.J. Sordalen,"Experimental Stabilization of Mobile Robots with Nonholonomic Constraints", *IEEE Trans.on Automatic Control*, Nov,1992 pp.1791-1797

[3] D. Necsulescu, A. Villien, M. Eghtesad,"Task Space Motion Control of Autonomous Planetary Vehicles", *8th CASI Conf. on Astronautics*, Ottawa, Canada, Nov 7-10, 1994, pp. 303-312.

[4] D. Necsulescu, M. Eghtesad, S. Kalaycioglu,"Dynamic Based Linearization and Control of an Autonomous Mobile Robot", *2nd Biennial European ASME Conf. on Engineering Systems Design & Analysis*, London, England, July 4-7, 1994.

[5] L. Del Re, J. Chapuis, V. Nevistie,"Predictive Control with Embedded Feedback Linearization for Bilinear Plants with Input Constraints", *Proc. CDC*, 1993, pp. 2984-2988

[6] *dSPACE Control and Development System*, Paderborn, Germany, 1989

[7] D. Necsulescu, B. Kim, S. Kalaycioglu,"Dynamics Control of an Autonomous Wheeled Ground Vehicle", *Trans. CSME*, Vol. 17, No. 4B, 1993, pp. 735-758